

Exploring Great Plains Nocturnal Low Level Jet Heterogeneity and Connections to Convection Initiation

MICHELLE R. SPENCER*

*National Weather Center Research Experiences for Undergraduates Program
Norman, Oklahoma*

ELIZABETH N. SMITH

*Cooperative Institute for Mesoscale Meteorological Studies, University of Oklahoma
and NOAA/OAR/National Severe Storms Laboratory
Norman, Oklahoma*

PETRA M. KLEIN

*School of Meteorology, University of Oklahoma
Norman, Oklahoma*

ABSTRACT

Observations from six nights of the 2015 Plains Elevated Convection At Night (PECAN) field campaign were used in this study to investigate the heterogeneity of the nocturnal low-level jet and draw possible connections between a heterogeneous jet and nocturnal convection initiation. The Great Plains region of the United States often experiences a nighttime precipitation maximum during the summer months, with some of the maximum being contributed to by convection that initiates overnight. Current understanding of the processes leading to nocturnal convection initiation is limited, but it is believed the nocturnal low-level jet may be playing an important role. The six cases chosen for this study showed clear diagonal striation signatures, suggesting the nocturnal low-level jet is heterogeneous in structure and the heterogeneity is much more common than previously thought. This signified a change in the structure of the nocturnal low-level jet and a missing component to past low-level jet climatologies. Additionally, a case study of one of the six cases showed evidence that the nocturnal low-level jet may be acting as a forcing mechanism for nocturnal convection initiation observed in the absence of other forcing mechanisms. The nocturnal low-level jet and its heterogeneous spatial-temporal evolution should be taken into consideration when forecasting for nocturnal convection initiation, especially in the absence of more traditional trigger mechanisms.

1. Introduction

The Great Plains region of the United States often experiences a nighttime maximum in boundary layer wind speed known as the nocturnal low-level jet (NLLJ). NLLJs typically occur in the lowest kilometer of the atmosphere as a result of nighttime decoupling of the surface layer and the boundary layer. During the day, a force balance is in place between the pressure gradient force, the Coriolis force, and the frictional force. As the surface cools after sunset, thermally-generated turbulence decays and a stable boundary layer (SBL) forms. The associated reduction in the frictional force eliminates the force balance that is present during the day, leading to an increase in wind speeds within the boundary layer. This effect causes an in-

terial oscillation, which is considered as a formation mechanism for NLLJs in the Great Plains of the United States (Blackadar 1957). While this study focuses on the Great Plains NLLJ, NLLJs have been documented in various places around the world including Australia and Africa (Brook 1985) and (Ardanuy 1979).

Climatological data has revealed a warm-season nocturnal maximum in precipitation in the Great Plains region, with an increase of nocturnal precipitation exceeding daytime precipitation by about 25% in the months of June-August (Higgins et al. 1997). This overnight maximum can be connected to frequent nocturnal convection both from persistence of daytime systems and from new nocturnal convection initiation (CI). In some cases, nocturnal CI occurs with little-to-no synoptic forcing present, suggesting other mechanisms must allow CI to occur in these

*Corresponding author address: Put your name, school affiliation and mailing address here (you may use CAPS address)
E-mail: mspenc25@msudenver.edu

environments. Here, we will explore the connection between the the NLLJ and nocturnal CI.

The Great Plains NLLJ plays an important role in transporting heat and moisture from the Gulf of Mexico into the central United States. This transport is important for supplying moisture to the interior portion of the continental United States, and also can be connected to the warm-season nocturnal precipitation maximum (Markowski and Richardson 2011). Additionally, the NLLJ has the ability to alter the dynamic and thermodynamic structure of the lower portions of the atmosphere. These changes in the lower atmosphere can often enhance the probability of convection initiation in the region. Convection that initiates overnight has the ability to be inherently more dangerous to the public, especially if the convection becomes severe in nature, making the importance of understanding the processes leading to nocturnal CI an important topic within the community.

Previous studies of the Great Plains NLLJ have been conducted in ways that are either spatially or temporally restricted. Bonner (1968) performed a two year climatological study of the NLLJ. While this study included two years worth of data, the data consisted of analysis of rawinsonde wind data from 0 UTC and 12 UTC. While the spatial extent of this study is good, the lack of observations when the NLLJ is at it's strongest leaves a gap in the temporal evolution of the jet. The study provided great insight to where the NLLJ occurs most frequently in the United States and at what height within the atmosphere, but the temporal resolution of the data was not sufficient for any conclusions about the temporal evolution of the jet during the night.

Whiteman et al. (1997) conducted a low-level jet climatology study based off of rawinsonde data that was obtained over a two-year period up to eight times a day, expanding on the work of Bonner 1968, but used only one location in north-central Oklahoma. The sounding analysis from this study provided a good source for the temporal evolution of the jet, but it was spatially limited leaving gaps in the evolution of NLLJ spatial characteristics.

Rife et al. (2010) conducted a study to investigate the characteristics of diurnally varying NLLJs using reanalysis data. While this study had a better temporal and spatial resolution of the jet, the study did not include observational data, and focused on defining bulk characteristics of NLLJs rather than internal spatial or temporal jet evolution. These limitations, again, allowed for missing areas of NLLJ evolution, both spatial and temporal.

These limitations have led the NLLJ to often be treated as a homogeneous structure. A less limited spatially and temporally study of the NLLJ is important to advance our knowledge of the processes associated with the NLLJ and what connections the jet may have to local nocturnal CI. In a recent study conducted by Smith et al. (2019),

the spatial evolution of the NLLJ was shown to be responsible for sudden changes in the local structure of the NLLJ, suggesting that the NLLJ is heterogeneous in nature. These sudden changes in structure included diagonal striation signatures in time-height wind profiles, veering winds with time and height, rising motion, and thermodynamic advection above the nose of the NLLJ. Additionally, Gebauer et al. (2018) investigated the connection between the changing structure of the NLLJ to CI within pristine environments. Gebauer et al. (2018) found that the heterogeneity of the NLLJ resulted in convergence of the u -wind component and that this convergence could have provided the lift needed for observed CI.

This study further investigates the heterogeneity of the NLLJ and how the NLLJ may enhance nighttime precipitation within the Great Plains through CI. The next section introduces the data used for this study, then observations are interpreted and discussed in section three. Section four investigates the connections of the heterogeneous NLLJ and nocturnal CI. Finally, section five summarizes this work and discusses future research.

2. Data and Methods

To explore the Great Plains nocturnal low-level jet and connections to convection initiation, this study used observation data from the Plains Elevated Convection At Night (PECAN) field campaign that took place between 1 June and 15 July 2015. The PECAN field campaign was an expansive project funded by The National Oceanic and Atmospheric Administration, the National Science Foundation, the National Aeronautics and Space Administration, and the Department of Energy (Geerts et al. 2017). The primary purpose of the project was to investigate and gain a better understanding of the processes that contribute to elevated nocturnal convection and the resultant nocturnal precipitation maximum over the Great Plains. To better understand these processes, four main targets were determined for detailed study and deployments: CI, bores, mesoscale convective systems, and NLLJs. Measurements and observations were taken by mobile and fixed PECAN Integrated Sounding Arrays (PISAs), with six Fixed PISAs (FPs) collecting data almost continuously and four Mobile PISAs (MPs) collecting data during Intensive Operational Periods (IOPs). All PISAs were equipped with some form of in-situ and remote sensing instrumentation. The locations of the FPs, the PECAN observational domain, and the topographical elevation of the domain can be seen in Fig. 1, while the MP locations varied depending on the IOP mission.

The most relevant sources of data for the present study include boundary layer profilers, which collect thermodynamic and kinematic observations. These observations are used to analyze the temporally-varying structure of the NLLJ and connections to NLLJ spatial evolution. High

temporal and vertical resolution data were collected using Atmospheric Emitted Radiance Interferometers (AERIs), Doppler lidars, radar wind profilers, and radiosondes. In addition to atmospheric profiling platforms, radar data were used to supplement the findings from the PECAN datasets.

After the relevant datasets were gathered, the PECAN observations were explored for cases of interest. Six cases were identified for further evaluation. It is important to note that these six cases were not evaluated in Smith et al. (2019) or Gebauer et al. (2018). While still using the PECAN dataset, this study focuses on cases that are less quiescent on the synoptic scale than the cases used in Smith et al. (2019) and Gebauer et al. (2018). This was a purposeful choice to allow for the evaluation of how common the features found in Smith et al. (2019) and Gebauer et al. (2018) are in more diverse meteorological environments. These cases fell on nights that had a mixture of IOP mission types, so the mobile units observation data varied in quality and availability. In most cases the FPs provided nearly continuous data collection. Summary information about each case included in this study is included in Table 1. No strong synoptic forcing and/or boundaries were present in these cases, such as strong synoptic-scale fronts or troughs. Weaker forms of boundaries, such as bores or stationary fronts, were observed on some of the nights, but we do not consider these features as strong, large-scale forcing. In fact, exploring cases with such features can offer insight into the complex interactions between heterogeneous NLLJs and mesoscale features, though that was not a direct focus in this study. NLLJs were observed by the PECAN network in all cases, and in most cases some form of convection initiation was identified in archived radar data.

One case, IOP 25, was well observed by all included FPs and MPs (for data relevancy purposes, FP1 was not included in these analyses). IOP 25 included strong signals of NLLJ heterogeneity and included CI, which occurred away from common initiation mechanisms. While all six cases are used for the investigation and evaluation of heterogeneous NLLJ structures, IOP 25 is used for analysis connecting NLLJ heterogeneity to CI. Time-height cross sections at different locations throughout the PECAN domain were used to analyze the spatial-temporal evolution and heterogeneity of observed NLLJs. Additional analyses including moisture advection tendencies at the PISA sites and soundings were used to assess the thermodynamic environments prior to the observed CI during IOP 25.

3. Observations of NLLJ Heterogeneity

Smith et al. (2019) documented that the heterogeneity of the NLLJ manifests itself in diagonal striation signatures when viewing single point observational data. The

diagonal striation signatures are what can be used to determine the heterogeneity of the NLLJ's spatial evolution throughout the night from PECAN's point observation data. Smith et al. (2019) found that multiple signatures suggest and result from the NLLJ's heterogeneity including; diagonal striation signatures in time-height vertical cross-sections of wind speed and wind direction, warm air advection (WAA) and moisture advection above the NLLJ with a strong westerly flow as the night progresses, and pulses of positive vertical motion found within the moving jet. To better explain the manifestation of these signatures, Smith et al. (2019) created a conceptual model of the spatial-temporal evolution of a heterogeneous NLLJ (2). In panel (a) at the beginning of the night, the strongest jet winds begin on the western slope, higher within the boundary layer. As the night progresses (b-c), the strongest jet winds move east and reach towards the surface as the jet advects itself down the slope of the Great Plains. The veering of the jet occurs in the same fashion. At the beginning of the evening (a) near the top of the jet, the u -component of the wind strengthens and leads to a more westerly wind component. As the night progresses (b-c), the veering of the winds advect east towards the surface. This heterogeneity leads to areas of enhanced speed and directional convergence within the moving jet. These convergence zones can be conducive to rising motion. Panel (d) shows how this spatial-temporal evolution of the heterogeneous NLLJ manifests in single point observational data like those used in this study. The time-height cross-section of wind speed and wind direction show diagonal striations as the jet advects itself down the slope of the Plains. In addition, the areas that are conducive to rising motion appear as small areas of observed positive vertical motion within vertical velocity time-height cross-sections. These small updrafts are important when taking into consideration the atmospheric conditions throughout the night and how elevated updrafts may play a role in boundary layer processes leading to the initiation of convection. Smith et al. (2019) also showed a connection between the increased westerly flow above the jet and an increase in potential temperature and changes in moisture via advection as the night progresses. These same signatures were noted in the works by Gebauer et al. (2018) as well. Both Gebauer et al. (2018) and Smith et al. (2019) investigated this heterogeneity of the NLLJ with a focus on synoptically quiescent nights, so this study builds off that previous work and looks into more synoptically complex cases to see if the same signatures are still in place.

a. Wind Speed

Examples of the diagonal striation signatures within the wind speed time-height cross-sections for each of the six cases chosen are shown in panel (a) of Figures 3 through

19. IOP 3 and IOP 5's observations are from FP3, while the remaining IOP observations include observational data from FP6. Since each case had a different setup and different data availability, it is not always practical or possible to show observations at the same site. In each of the six cases, the diagonal striation signatures described by Smith et al. (2019) are clearly visible from at least one of the data observation sites. Each case illustrates that increased wind speeds occur near the top of the NLLJ, before deepening and reaching closer to the surface as the night progresses. These time-height cross-sections of the observed wind speed all occurred on nights with varying synoptic setups. As pointed out in previous work, these striations can be a manifestation of NLLJ spatial heterogeneity in a local point-observation time series. The evidence of the heterogeneity of each jet, regardless of the synoptic setup, is an interesting observation and important result of this work. The heterogeneity of the wind speed also shows evidence of the possibility of enhanced wind speed convergence areas within the jet, with faster speeds being advected down the slope into areas of lower speeds.

b. Wind Direction

The heterogeneity of the NLLJ can also be observed by viewing the time-height cross-sections of wind direction from single point observation sites. The long accepted theory of the NLLJ tells us that the jet will veer overnight (e.g., Blackadar 1957). Since previous studies treated the NLLJ as a homogeneous structure, the veering was often assumed to happen everywhere over the same time period. However, the work done by Smith et al. (2019) has shown that the heterogeneous jet's spatial evolution manifests itself in the diagonal striation signatures seen in panel (b) of figures 3 through 19. The veering of the winds first occurs in the region above the core of the NLLJ and it coincides with the increased wind speeds. The associated increase in the u -component of the wind can lead to non-linear advection of the NLLJ down the slope of the Great Plains (via the $u \frac{\partial u}{\partial t}$ advection term). In each of the six cases, the winds veer, but as the night progresses the veering winds advect the jet down the slope (strongest NLLJ winds occur earlier in the west and later in the east, not shown) and the veering deepens within the boundary layer. This spatial-temporal veering means that local changes in wind direction could lead to local zones conducive to convergence. These changes of the NLLJ structure and the resultant enhanced convergence potential could be enough to initiate elevated convection if the atmospheric conditions are in place for initiation of convection. This is different to the more typical consideration of NLLJ related CI occurring in so-called 'terminus' zones on the northern and/or eastern edges of the NLLJ. The heterogeneous NLLJ could

have the ability to initiate convection outside of the terminus zone and within the jet itself, depending on the existing atmospheric conditions.

c. Vertical Motion

Associated with the spatial-temporal veering and increase of wind speed discussed above, heterogeneous NLLJs have been shown to be supportive of localized bursts of vertical motion (Smith et al. 2019). As shown in the conceptual model, as heterogeneities in the spatial NLLJ structure move with the advection of the jet down the slope speed and directional convergence associated with the changes within the jet structure can lead to areas of enhanced convergence potential. The enhanced convergence potential leads to areas that are conducive to positive vertical motion and updrafts, which can be seen in point-observations.

Similar instances of sudden vertical motion were found in the cases included in this study, despite the differences in synoptic conditions in cases included in Smith et al. (2019). These pulses of positive vertical motion can be seen in Figures 3 through 19. A clear example of this signature can be seen in Figure 3 (c) which shows three areas between 8 UTC and 10 UTC with relatively strong positive vertical motions. A closer look at the wind speed and wind direction at this time (Fig. 3 (a) and (b)) reveal coincident strong striation signatures, suggesting the vertical motions are related to localized changes within the NLLJ structure caused by the heterogeneity of the jet. In the cases used for this study, evidence of positive vertical motion is observed in nearly every case and helps solidify the conceptual model of Smith et al. (2019).

d. Thermodynamic Advection

As suggested in the previous study by Smith et al. (2019), the spatial-temporal evolution of the heterogeneous NLLJ would also impact advection of thermodynamic properties along the slope of the Great Plains. As the NLLJ veers with time and height, the increased u -component can act to advect heat and moisture down the slope. As such, warmer environmental potential temperature is often brought down the slope by the increased u -component, and manifests locally as warming above the NLLJ nose. This warming above the NLLJ maximum paired with expected cooling in the stable surface layer results in increased static stability in the layer where the NLLJ exists. Through similar mechanisms, zones of dry or moist air can be advected from west to east as shown in Smith et al. (2019), though in more complex environments this feature is more difficult to diagnose. The expected warming above the NLLJ is seen in nearly every case (Figs. 3 through 19). As an example, Figure 17 illustrates the warming that occurs as the night progresses and the higher potential temperature is advected down the

slope. At this same time, the slope's surface continues to cool, increasing the static stability in the boundary layer.

4. Connections between Heterogeneous NLLJs and Nocturnal CI

IOP 25 took place on 11 July with mobile units collecting observations from approximately 0000-0930 UTC. The synoptic conditions at 0 UTC included a weak stationary front (Fig. 20) that was oriented in a mostly east-west direction along the northern border of Kansas, dipping slightly south around the central northern border of Kansas. At approximately 3 UTC the NLLJ begins to form in the higher regions of the boundary layer at most of the observation sites. As the night progresses the stationary front shifts to the north and the automated classification provided by the Weather Prediction Center now analyzes it as a warm front (Fig. 20). Since the NLLJ is active during the night, this re-classification by the objective algorithm likely is a result of warm southerly flow associated with the NLLJ itself. This type of synoptic setup is considerably different than the synoptic setups used in Gebauer et al. (2018), which included cases with more synoptically quiescent conditions. The CI that occurred during IOP 25 apparently took place in what is often called a "pristine" environment, meaning traditional forcing such as an outflow or frontal boundary is not present in the immediate region.

The night of IOP 25 was declared as a bore mission for PECAN operations, and the four mobile units were in place throughout north central Kansas to await the development and passage of a bore associated with expected convection to the north. By 4 UTC a mesoscale convection complex was located just east of McCook, Nebraska, but dissipated as it moved east-southeast (Fig. 20). A bore-like structure was observed by the PECAN assets south of this system in the hours following. The north to south progression of the bore-like structure is seen in radar images between 8 UTC and 10 UTC in north central Kansas (Fig. 21). By approximately 1125 UTC, CI was detected via radar to the north of Topeka, Kansas (Fig. 21). A northward moving feature was also detected at this time, to the west of where the CI occurred and north of the bore, near Hays, Kansas. The location of the CI is well away from any obvious detected phenomena that could act as possible drivers for the convection.

While observation plans were intended to capture bore-associated phenomena, the PECAN assets also observed a NLLJ during the night of IOP 25. NLLJ observations were collected at each MP and FP location shown in Figure 20. FP6 and MP4 were the closest observation sites to where the CI occurred; however, MP4 did not collect data after about 430 UTC, so observations from FP6 will be shown for the remainder of this case's analysis.

Figure 9 (a) and (b) show the diagonal striation signatures discussed in previous sections, suggesting spatially heterogeneous NLLJ structure. If we rely on the Smith et al. (2019) conceptual model, then we can expect the heterogeneity of the jet to create areas of increased potential for convergence due to the temporal evolution of the u -component of the wind. The diagonal striation in the wind speed profiles and the veering in time and height shown in the wind direction profiles observed at FP6 indicated an area at about 600 meters above ground level around 9 UTC where positive vertical motion could have existed (Fig. 13 (a) and (b)). During and after the passage of signatures related to the NLLJ heterogeneity in the wind speed and direction profiles (between 9 UTC and 930 UTC) the vertical velocity observations at FP6 show multiple instances of sudden upward motion (Fig. 13 (c)). This enhanced convergence potential and evidence of upward vertical motion could have been an important factor in the observed CI, in the absence of other forcing mechanisms.

Two soundings in the general region around the CI were launched between 08 and 12 UTC: PECAN sounding from MP4 at 0850 UTC (Fig. 23) and operational sounding from Topeka at 1200 UTC (Fig. 24). Skew-T analysis of these two soundings indicates a destabilization within the lower atmosphere above the surface layer. The MP4 sounding, which was located to the north west of the CI area, showed a very shallow layer of moisture, and thus relatively little and hard to realize elevated convective available potential energy (CAPE). By 12 UTC, the sounding launched from Topeka, Kansas (south west of the CI area) indicated a deeper elevated moist layer, steeper lapse rates above the surface layer, and thus more CAPE that could be realized if an elevated parcel was lifted through the atmosphere. This analysis suggests that moisture increase and temperature advection, both possibly associated with the jet itself, increased the elevated instability in the region where CI would later occur.

If the CI region's environment was otherwise primed for convection potential, and a heterogeneous NLLJ with localized regions conducive to convergence was acting in this environment, the aforementioned vertical motion that can be driven by the jet could have been enough to displace elevated air parcels and initiate the convection. However, this can not be proven based from PECAN observational data alone. Even with the generally unprecedented spatial and temporal resolution of the PECAN boundary layer observations, there are still large areas where no observations were collected. Additionally, mobile observations ended before the CI occurred on this night. To make a determination about what drivers caused the convection initiation observed during IOP 25, additional analysis methods are required including analysis of operational model reanalysis and numerical simulation studies of this event. With numerical weather prediction tools, the hypotheses laid out above could be further evaluated and tested to establish

the role of NLLJ heterogeneity in this case of convection initiation. Without those tools, we can only hypothesize that NLLJ heterogeneity could provide enough forcing to initiate convection in this case.

5. Summary and Discussion

The Great Plains region of the United States often experiences a nighttime maximum in precipitation. The same area is also often under the influence of the NLLJ. The previous studies of NLLJs have often been either spatially or temporally limited, leading the jet to be treated as a homogeneous structure. The recent works by Smith et al. (2019) and Gebauer et al. (2018) have extended our understanding by finding evidence that the jet structure is actually heterogeneous. The spatial heterogeneity of the jet was shown to manifest itself in local NLLJ structure via diagonal striation signatures. These important findings have highlighted a gap in the climatologies of the NLLJ and have led to new questions about the NLLJ's role in nocturnal CI. Gebauer et al. (2018) showed evidence that the NLLJ may be responsible for nocturnal CI in areas outside of the previously studied 'terminus' zones that are associated with the NLLJ. Since the atmospheric science community's knowledge of the processes leading to nocturnal CI is limited, a better understanding of the NLLJ may help to advance our understanding of different processes leading to the CI.

This study further investigated the heterogeneity of the NLLJ and the possible role the NLLJ may be playing in nocturnal CI. Observational data was used from the PECAN field campaign that took place from 1 June through 15 July of 2015. The field campaign provided an unprecedented amount of data collection of nighttime phenomenon, including NLLJs. A variety of instruments were used that were capable of sampling the boundary layer. Six NLLJ cases were chosen from the field campaign for study. The six cases included three criteria; an observed NLLJ, CI occurrence, and the absence of strong synoptic forcing features.

The analysis of numerous locations throughout the PECAN field campaign domain showed evidence that the NLLJ is heterogeneous in nature. Smith et al. (2019) found that the spatial heterogeneity of the NLLJ can be seen in single point observational data of wind speed and wind direction via diagonal striation signatures. Additionally, WAA in the area above the jet with strong westerly flow and areas of sudden pulses of positive vertical motion were also identified by Smith et al. (2019) as evidence of a heterogeneous NLLJ. Gebauer et al. (2018) found the same evidence of the heterogeneity of the NLLJ in his study, connecting the heterogeneity to the CI that occurred in pristine environments on several nights during the PECAN campaign. These same signatures found by Smith et al. (2019) and Gebauer et al. (2018) were found

in each of the six cases chosen for this study. Smith et al. (2019) only analyzed cases in which the PECAN IOP were deployed for NLLJ setup, meaning that the synoptic conditions were quiescent and no convection was expected and Gebauer et al. (2018) analyzed cases where CI occurred, but only in pristine environments. The combination of the six cases in this study and the cases used in Smith et al. (2019) and Gebauer et al. (2018) work suggest that the heterogeneity of the NLLJ is a much more common feature than previously thought. While Smith et al. (2019) identified the signatures that point to the heterogeneity of the NLLJ and Gebauer et al. (2018) analyzed cases of CI occurrence in pristine environments, this study looked into cases that were more complex in dynamic and thermodynamic structure.

Since the same signatures were observed on nights with the complex atmospheric conditions, the heterogeneity of the jet appears to be a common feature. This finding suggests that our existing NLLJ climatology may be missing an important aspect of the jet. The localized changes within the NLLJ could be playing important roles in nocturnal CI that is common during the summer months in the Great Plains region. Additional studies of both observational and model datasets are needed to quantify these effects and update our climatological understanding accordingly.

In the case of IOP 25, the NLLJ could have been the forcing mechanism for the observed CI. IOP 25 was originally a bore mission for the PECAN scientists, but this allowed for good data collection of the NLLJ over many areas within the domain. A weak warm front (previously analyzed as a stationary front) was present to the north of the Kansas border around the time the CI was detected via radar. The frontal boundary was far enough away from the CI that it is not believed it played a role in triggering the convection, nor was any other obvious trigger present in the surrounding area. Sounding analysis of the surrounding area showed an increase in moisture content and enough instability present within the atmosphere to be conducive to convection, if air parcels could be lifted. The NLLJ observed on this night showed all the heterogeneous signatures and positive vertical motions were observed near the time of the nocturnal CI. This suggests that the NLLJ could have acted as the lifting mechanism needed for the CAPE to be realized and for CI to occur and maintain itself. The combination of the heterogeneous NLLJ, enhanced convergence potential, and destabilization of the environment, likely contributed to the initiation of the convection. This is crucial in our understanding of what processes could be leading to nocturnal CI. However, no definitive conclusion can be made based solely off these PECAN observational data.

In order to better investigate the connections between the NLLJ and in nocturnal CI during IOP 25, simulation and/or reanalysis data would need to be analyzed. The

simulation and reanalysis data would help to identify if the jet was responsible for water vapor transport and how the jet affected the stability of the atmosphere on this night. The investigation into the reanalysis and simulation data would help to solidify the hypothesis that the NLLJ is a likely component to nocturnal CI.

Despite not being able to definitively state that the NLLJ was responsible for the observed CI in the case considered here, there is substantial evidence to suggest the jet should be viewed as a potential driver for convection that initiates overnight in the absence of other forcing mechanisms. This is especially true for NLLJ regions beyond the often studied terminus zone. This study showed, in addition to Smith et al. (2019) and Gebauer et al. (2018), evidence that the heterogeneity of the NLLJ is a much more common feature than previously thought. The associated changes to the boundary layer caused by the heterogeneity supports the hypothesis that there are areas within the jet that have the possibility to be conducive to enhanced convergence. These convergence zones could be enough of a source of lift to displace parcels so that the instability within the atmosphere can be realized.

The nocturnal maximum in precipitation during the summer months over the Great Plains is still a question that atmospheric scientists are struggling to unravel and answer. This important component could help to fill in some of the gray areas where our understanding of the boundary layer processes and NLLJ influence are lacking. By viewing reanalysis data and simulation data, we could address the questions of if the NLLJ is a cause of CI, if nocturnal CI can be attributed to the NLLJ alone, and how NLLJs should be considered when forecasting for nocturnal CI.

Acknowledgments

This research was completed with support by the National Science Foundation under Grant AGS-1560419. The authors acknowledge the participants in the PECAN field campaign for the observational data used in this work. The authors are grateful to Josh Gebauer and Tyler Bell for their aid with python related difficulties in producing figures. Finally, appreciation is extended to Dr. Daphne LaDue (Center for Analysis and Prediction of Storms, University of Oklahoma) and her associates for the coordination of the Research Experience for Undergraduates and for providing support, guidance, and advice throughout the course of the project.

References

- Ardanuy, P., 1979: On the observed diurnal oscillation of the Somali jet. *Monthly Weather Review*, **107** (12), 1694–1700.
- Blackadar, A. K., 1957: Boundary layer wind maxima and their significance for the growth of nocturnal inversions. *Bulletin of the American Meteorological Society*, **38** (5), 283–290.
- Bonner, W. D., 1968: Climatology of the low level jet. *Monthly Weather Review*, **96** (12), 833–850.
- Brook, R., 1985: The Koorin nocturnal low-level jet. *Boundary-Layer Meteorology*, **32** (2), 133–154.
- Gebauer, J. G., A. Shapiro, E. Fedorovich, and P. Klein, 2018: Convection initiation caused by heterogeneous low-level jets over the Great Plains. *Monthly Weather Review*, **146** (8), 2615–2637, doi:10.1175/MWR-D-18-0002.1.
- Geerts, B., and Coauthors, 2017: The 2015 Plains Elevated Convection At Night field project. *Bulletin of the American Meteorological Society*, **98** (4), 767–786, doi:10.1175/BAMS-D-15-00257.1.
- Higgins, R., Y. Yao, E. Yarosh, J. E. Janowiak, and K. Mo, 1997: Influence of the Great Plains low-level jet on summertime precipitation and moisture transport over the central United States. *Journal of Climate*, **10** (3), 481–507.
- Markowski, P., and Y. Richardson, 2011: *Mesoscale meteorology in midlatitudes*, Vol. 2. John Wiley & Sons.
- Rife, D. L., J. O. Pinto, A. J. Monaghan, C. A. Davis, and J. R. Hannan, 2010: Global distribution and characteristics of diurnally varying low-level jets. *Journal of Climate*, **23** (19), 5041–5064.
- Smith, E. N., J. G. Gebauer, P. M. Klein, E. Fedorovich, and J. A. Gibbs, 2019: The Great Plains low-level jet during PECAN: Observed and simulated characteristics. *Monthly Weather Review*, **147** (6), 1845–1869, doi:10.1175/MWR-D-18-0293.1.
- Whiteman, C. D., X. Bian, and S. Zhong, 1997: Low-level jet climatology from enhanced rawinsonde observations at a site in the southern Great Plains. *Journal of Applied Meteorology*, **36** (10), 1363–1376.

TABLE 1. Summary information about each of the six PECAN cases included in this study are shown in this table.

Date/IOP	NLLJ	Large-Scale Forcing	CI
6-5/03	Clearly Observed	Clearly Observed	Observed
6-6/05	Observed	Observed	Observed
7-11/25	Clearly Observed	Clearly Observed	Clearly Observed
7-12/26	Clearly Observed	None	Observed
7-13/27	Partially Observed	Partially Observed	Clearly Observed
7-16/31	Observed	Observed	Partially Observed

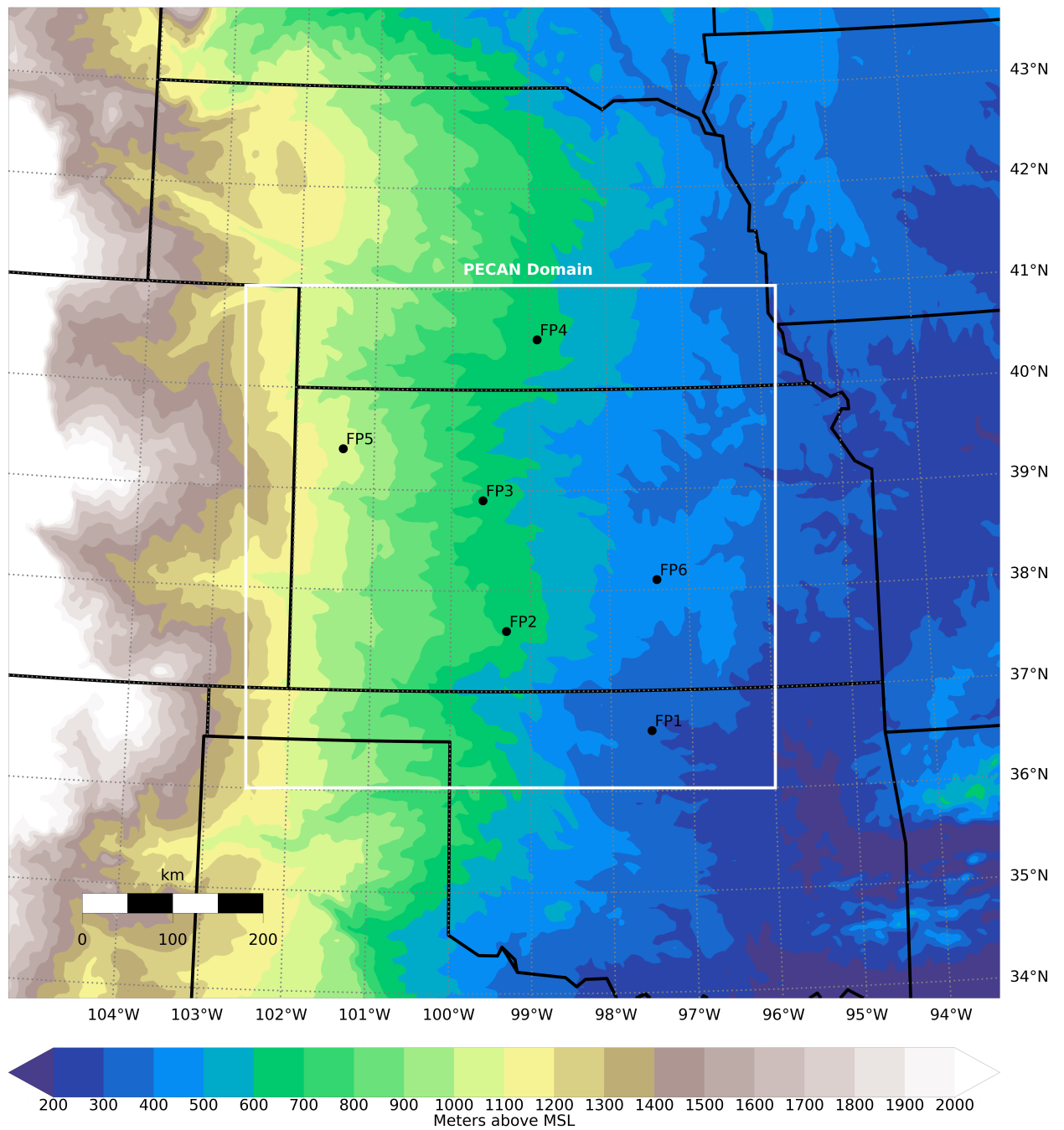


FIG. 1. Geographical representation of the observational PECAN domain and the FP locations.

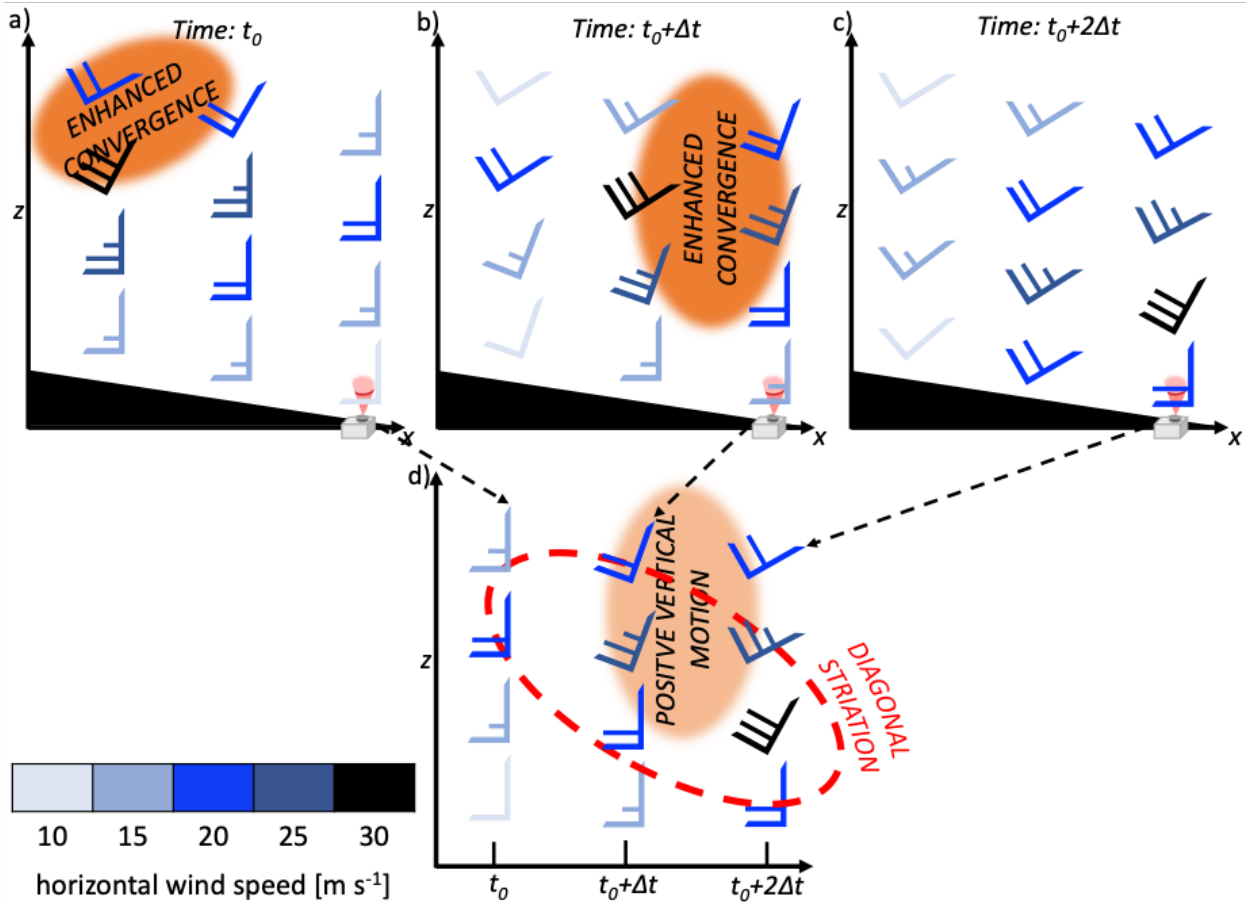


FIG. 2. Conceptual model created by Smith et al. (2019) depicting the evolution of the heterogeneous NLLJ across the slope (a-c) and the resulting profile observation (d).

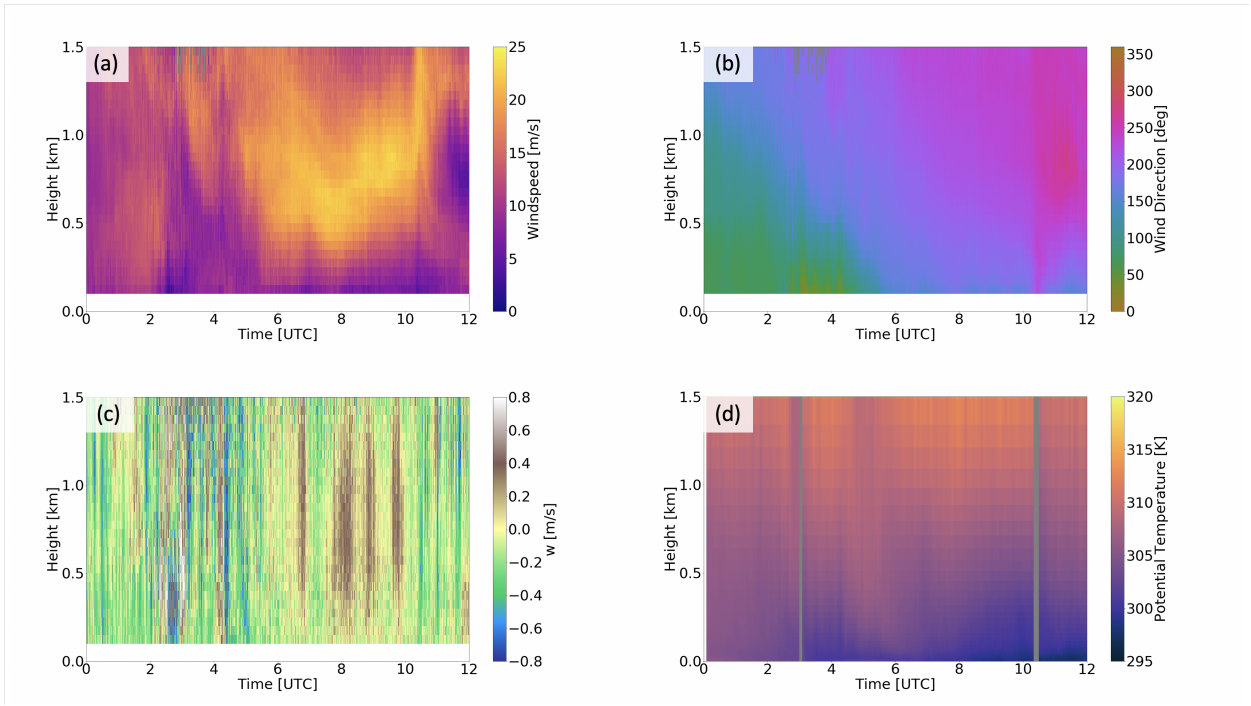


FIG. 3. Time-height cross sections of wind speed (a), wind direction (b), vertical velocity (c), and potential temperature (d) during IOP 3 at FP3.

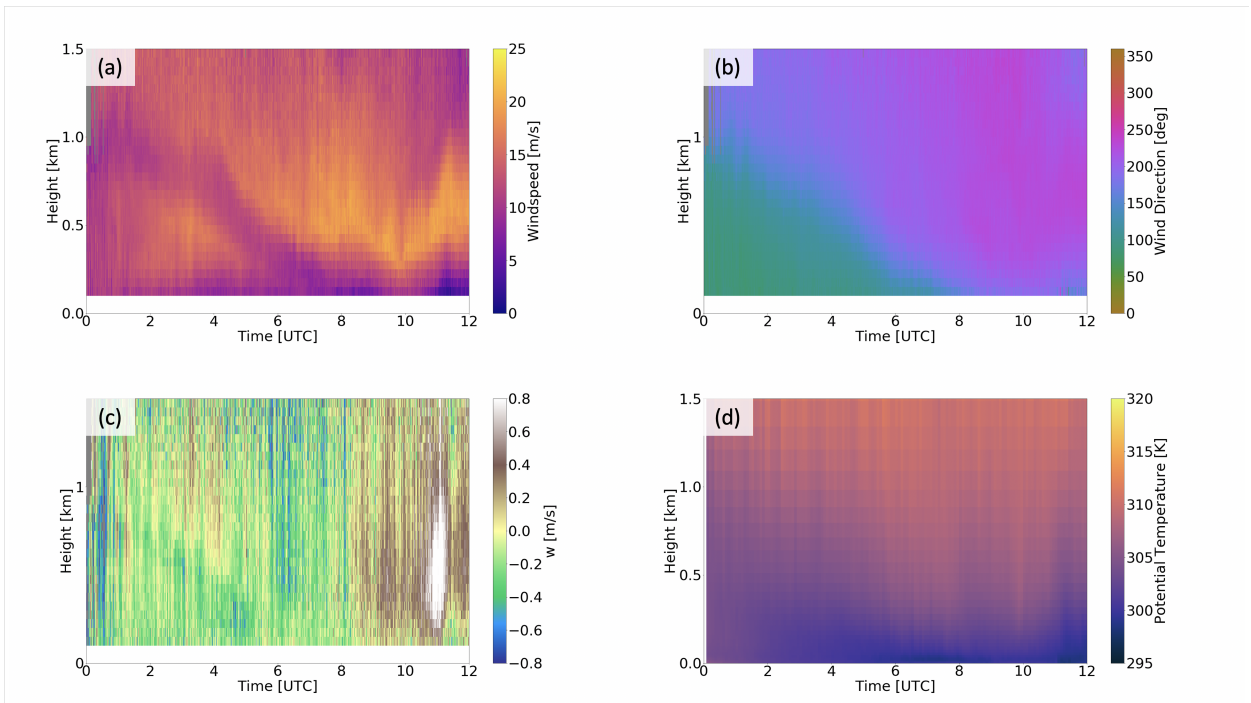


FIG. 4. Time-height cross sections of wind speed (a), wind direction (b), vertical velocity (c), and potential temperature (d) during IOP 5 at FP3.

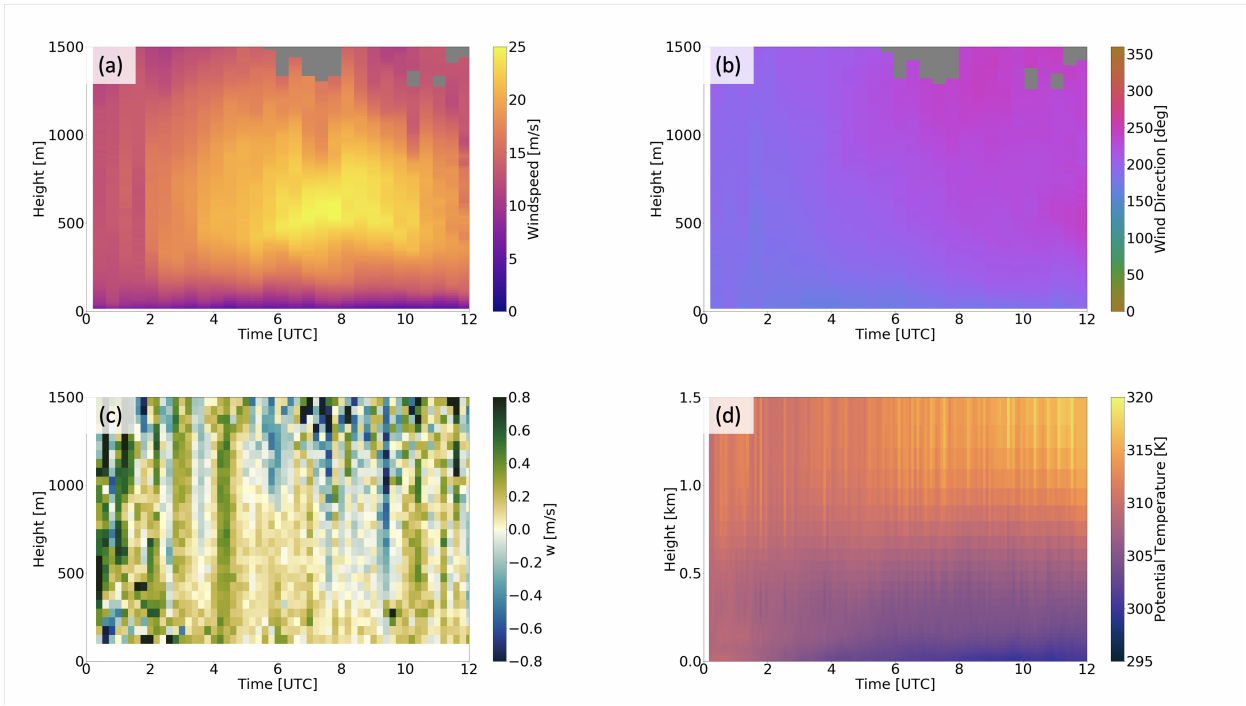


FIG. 5. Time-height cross sections of wind speed (a), wind direction (b), vertical velocity (c), and potential temperature (d) during IOP 25 at FP2.

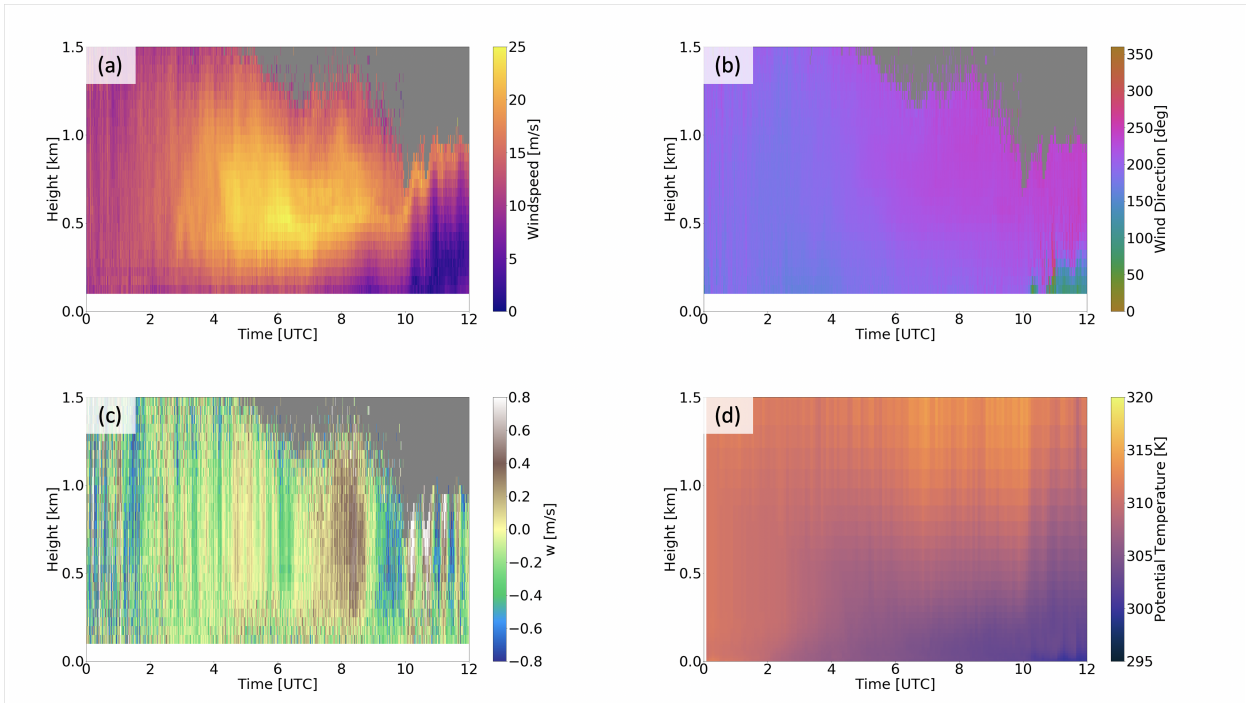


FIG. 6. Time-height cross sections of wind speed (a), wind direction (b), vertical velocity (c), and potential temperature (d) during IOP 25 at FP3.

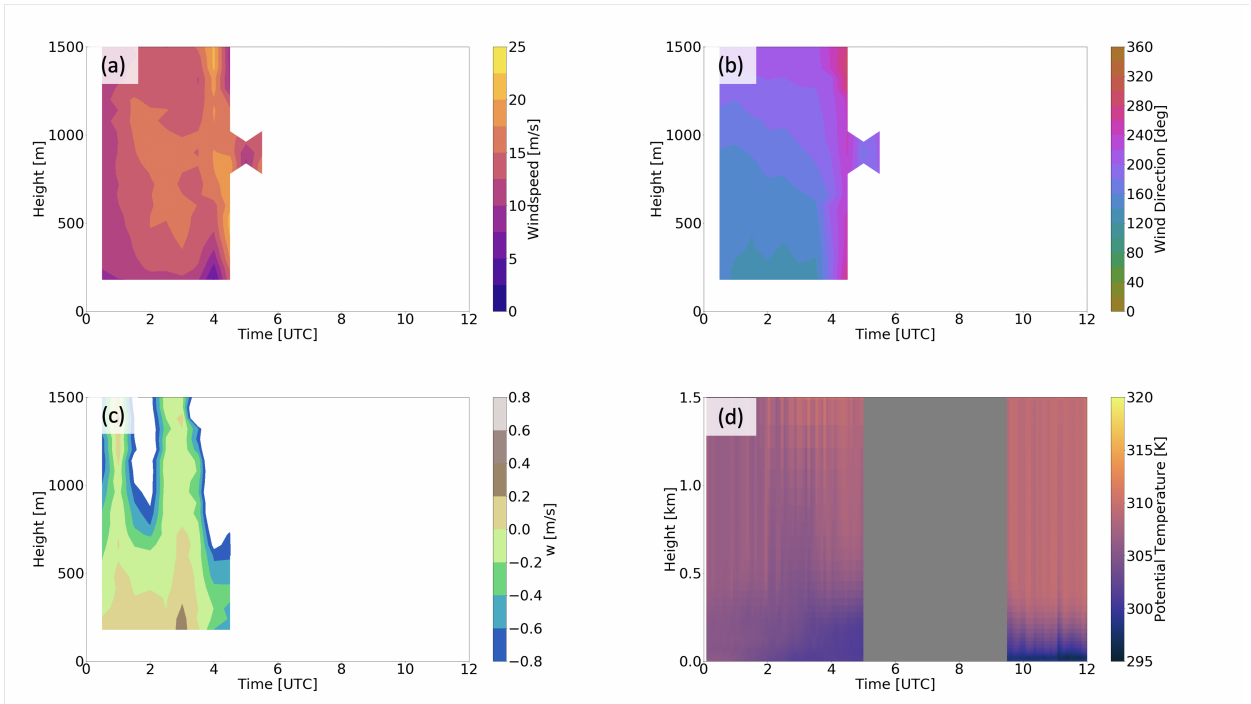


FIG. 7. Time-height cross sections of wind speed (a), wind direction (b), vertical velocity (c), and potential temperature (d) during IOP 25 at FP4.

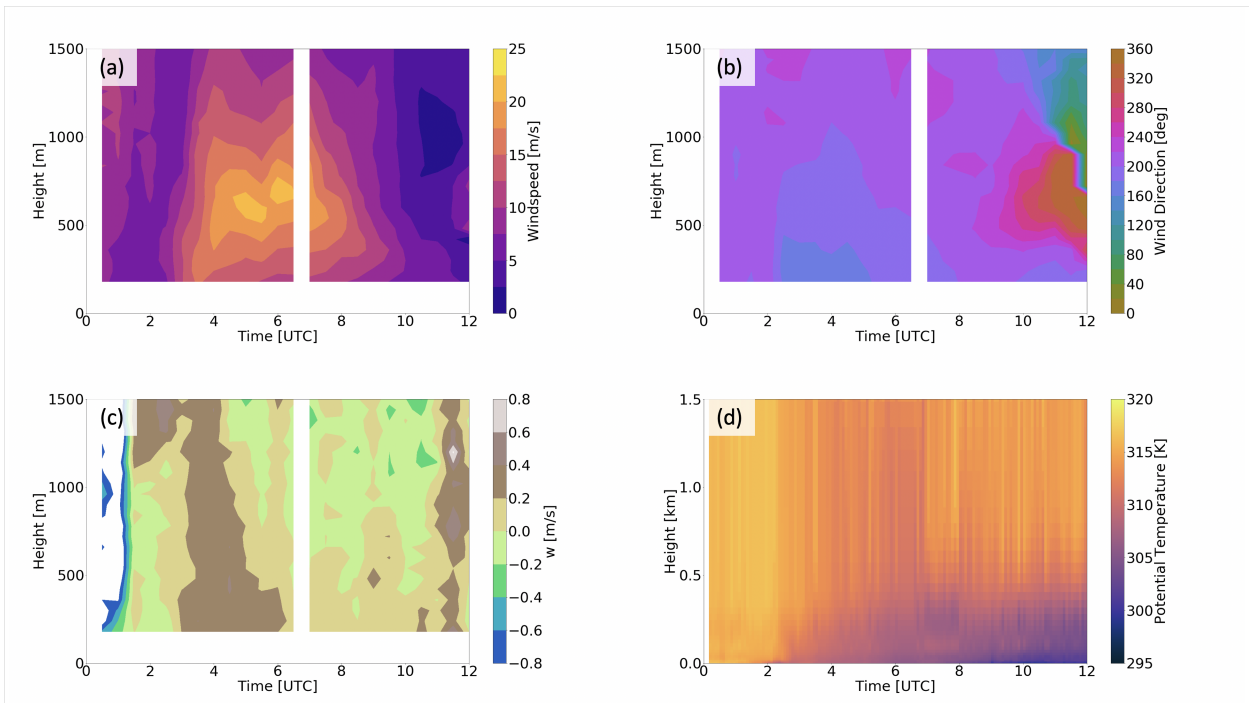


FIG. 8. Time-height cross sections of wind speed (a), wind direction (b), vertical velocity (c), and potential temperature (d) during IOP 25 at FP5.

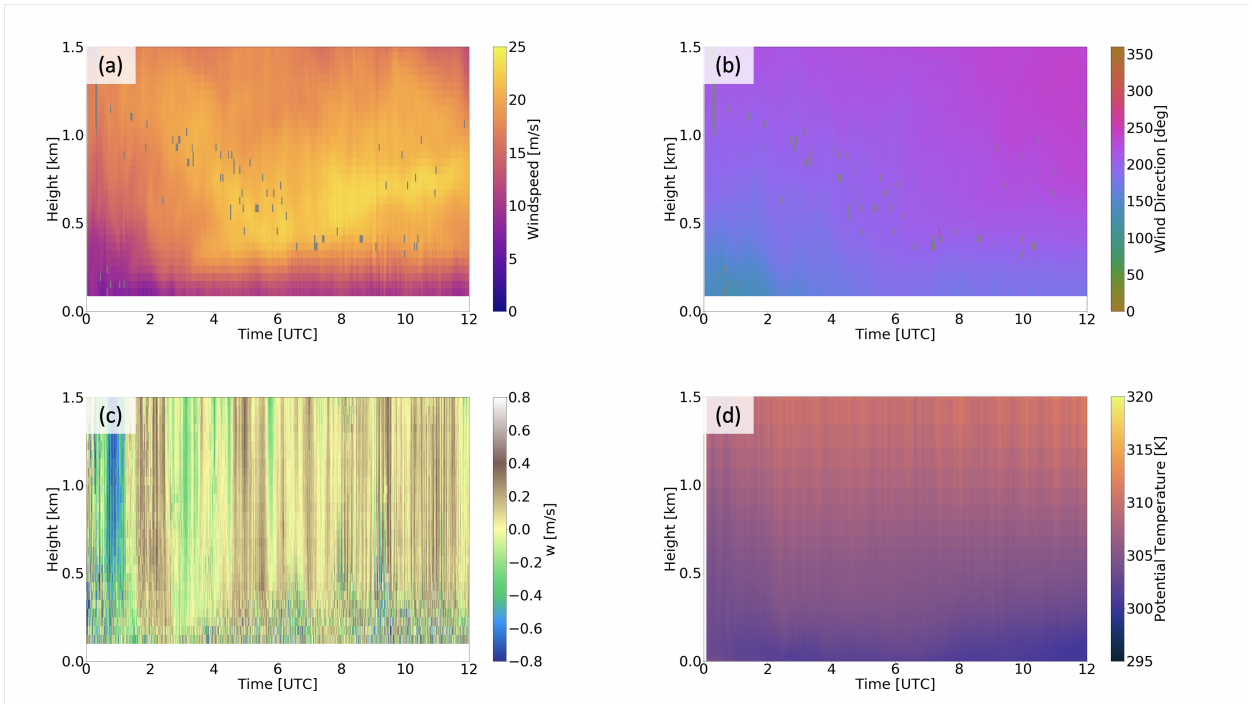


FIG. 9. Time-height cross sections of wind speed (a), wind direction (b), vertical velocity (c), and potential temperature (d) during IOP 25 at FP6.

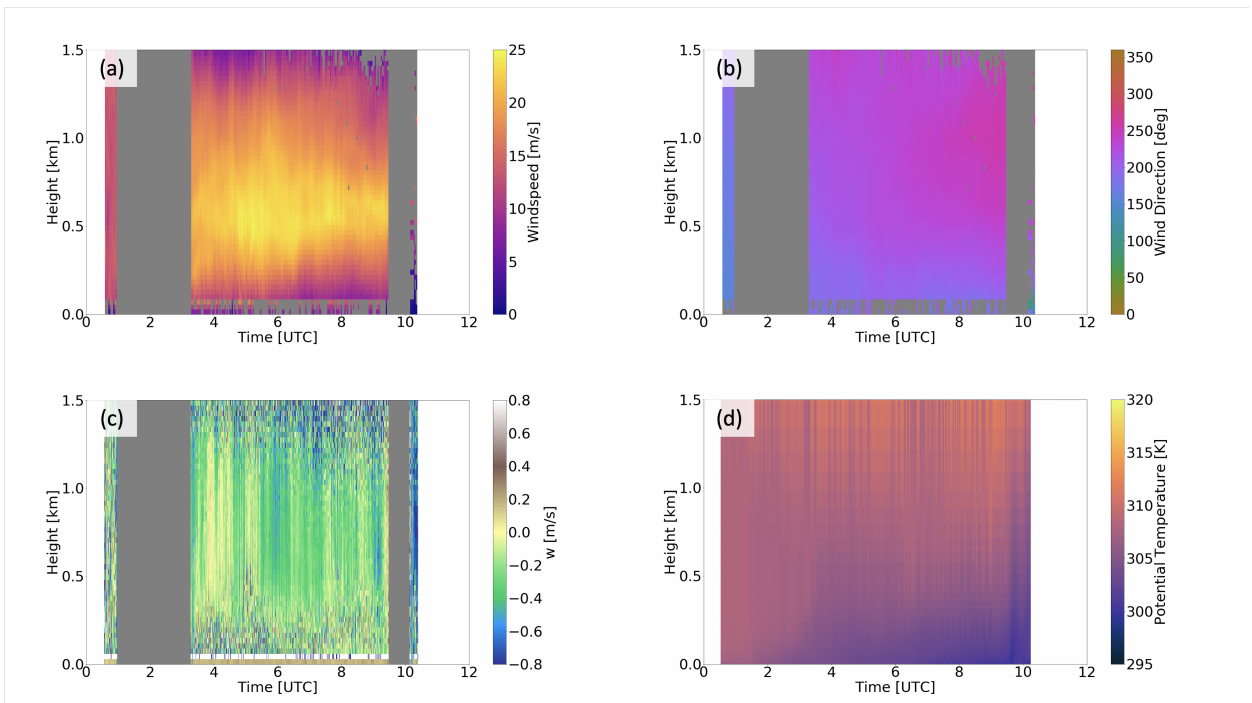


FIG. 10. Time-height cross sections of wind speed (a), wind direction (b), vertical velocity (c), and potential temperature (d) during IOP 25 at MPI.

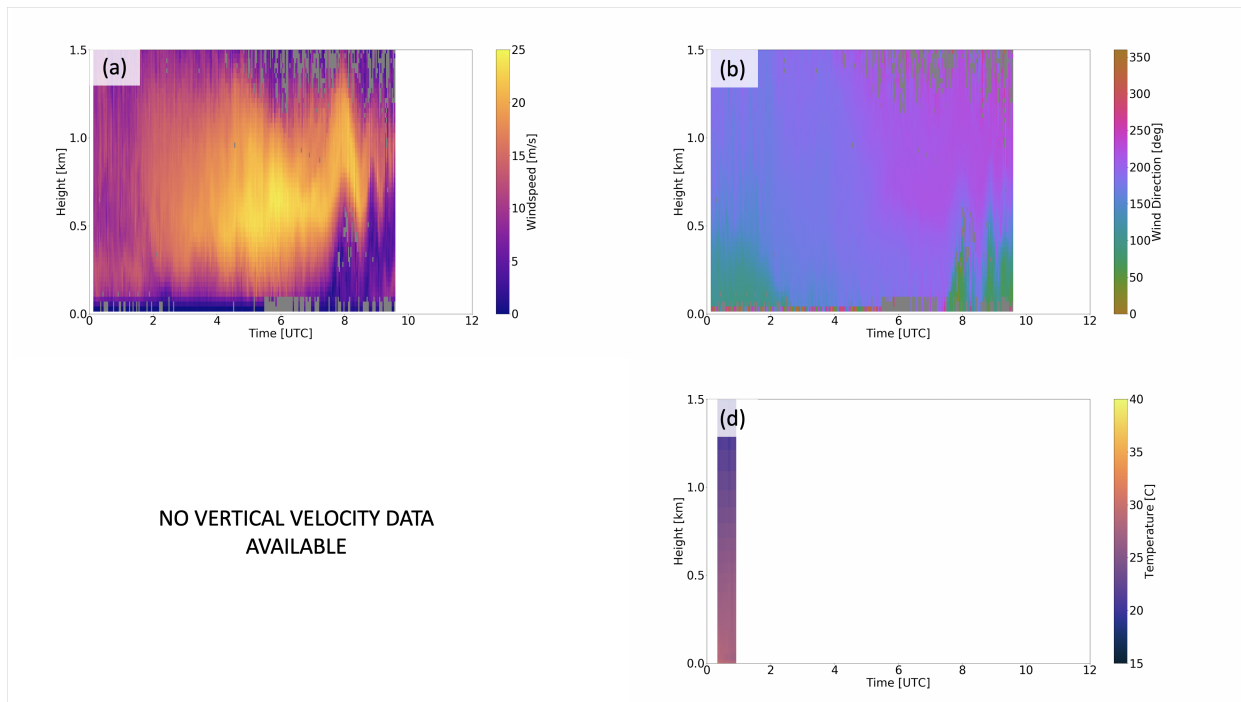


FIG. 11. Time-height cross sections of wind speed (a), wind direction (b), vertical velocity (c), and potential temperature (d) during IOP 25 at MP3.

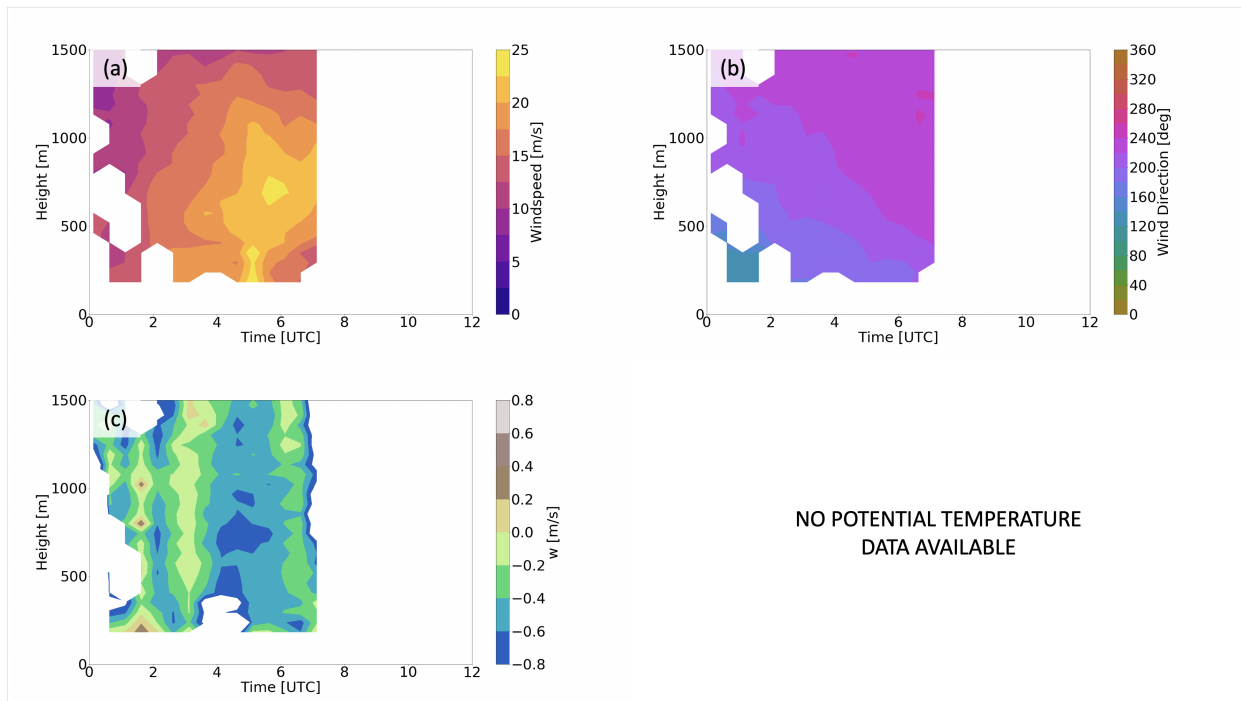


FIG. 12. Time-height cross sections of wind speed (a), wind direction (b), vertical velocity (c), and potential temperature (d) during IOP 25 at MP4.

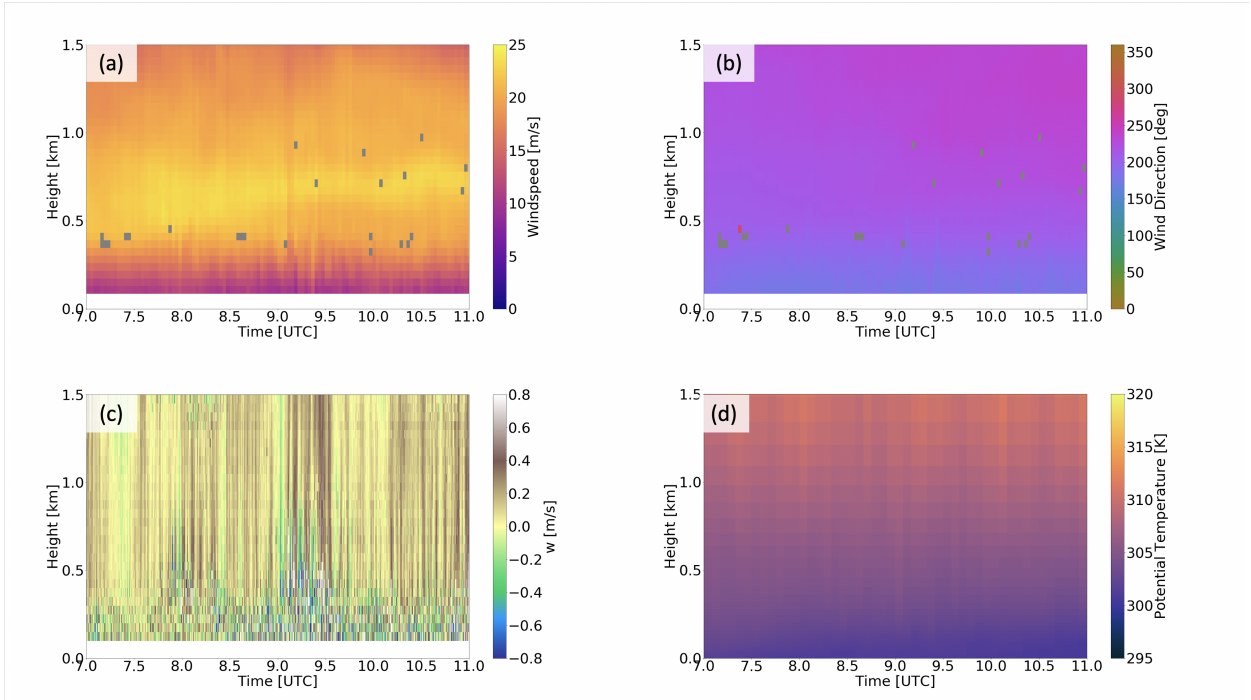


FIG. 13. Time-height cross sections of wind speed (a), wind direction (b), vertical velocity (c), and potential temperature (d) during IOP 25 at FP6 from 7UTC till 11UTC.

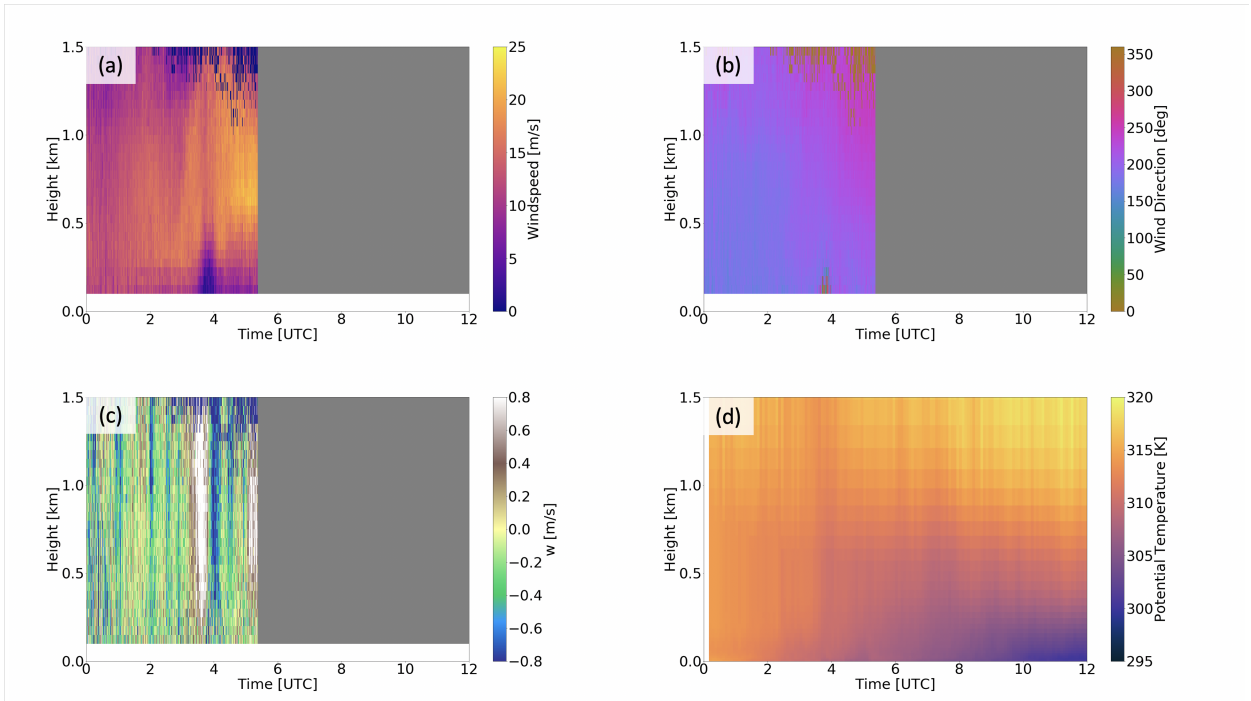


FIG. 14. Time-height cross sections of wind speed (a), wind direction (b), vertical velocity (c), and potential temperature (d) during IOP 26 at FP3.

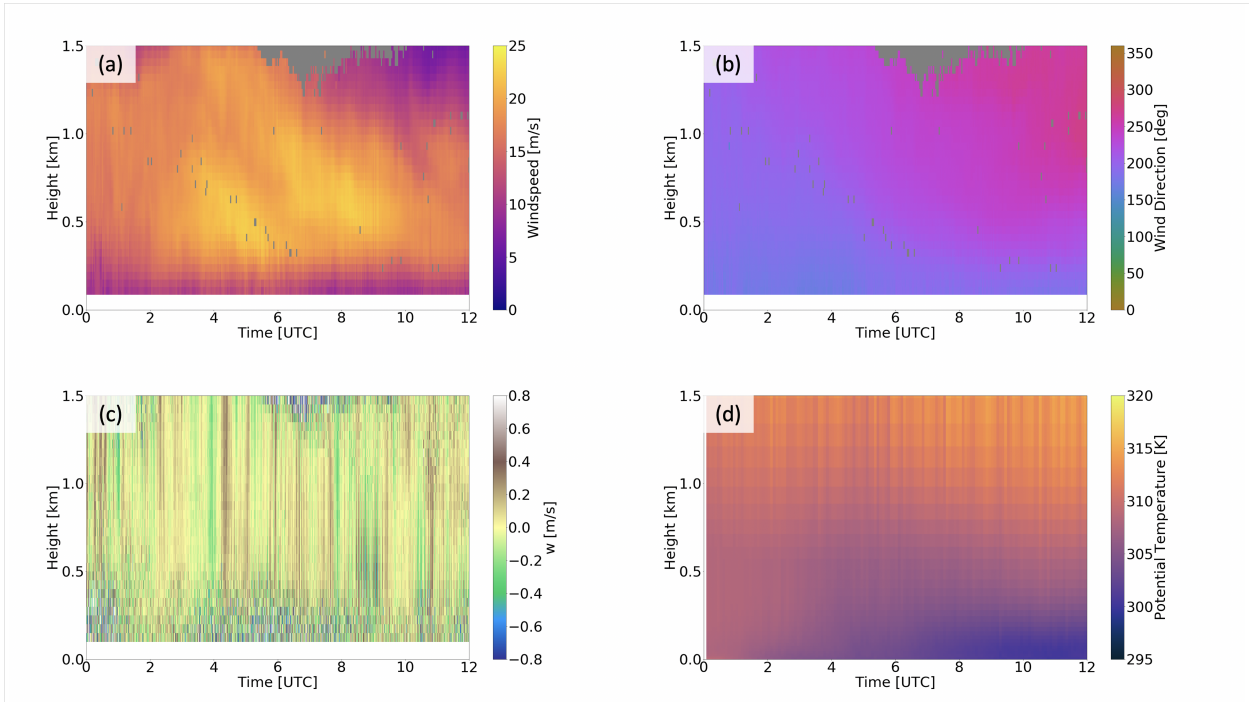


FIG. 15. Time-height cross sections of wind speed (a), wind direction (b), vertical velocity (c), and potential temperature (d) during IOP 26 at FP6.

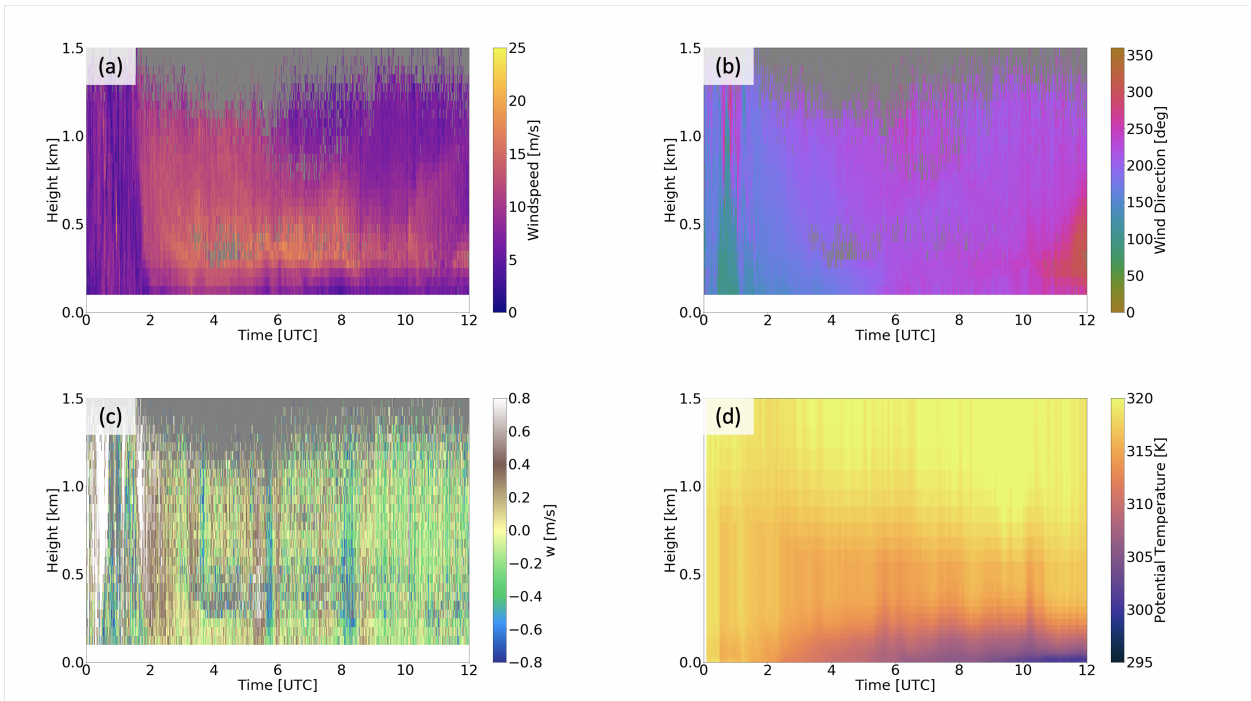


FIG. 16. Time-height cross sections of wind speed (a), wind direction (b), vertical velocity (c), and potential temperature (d) during IOP 27 at FP3.

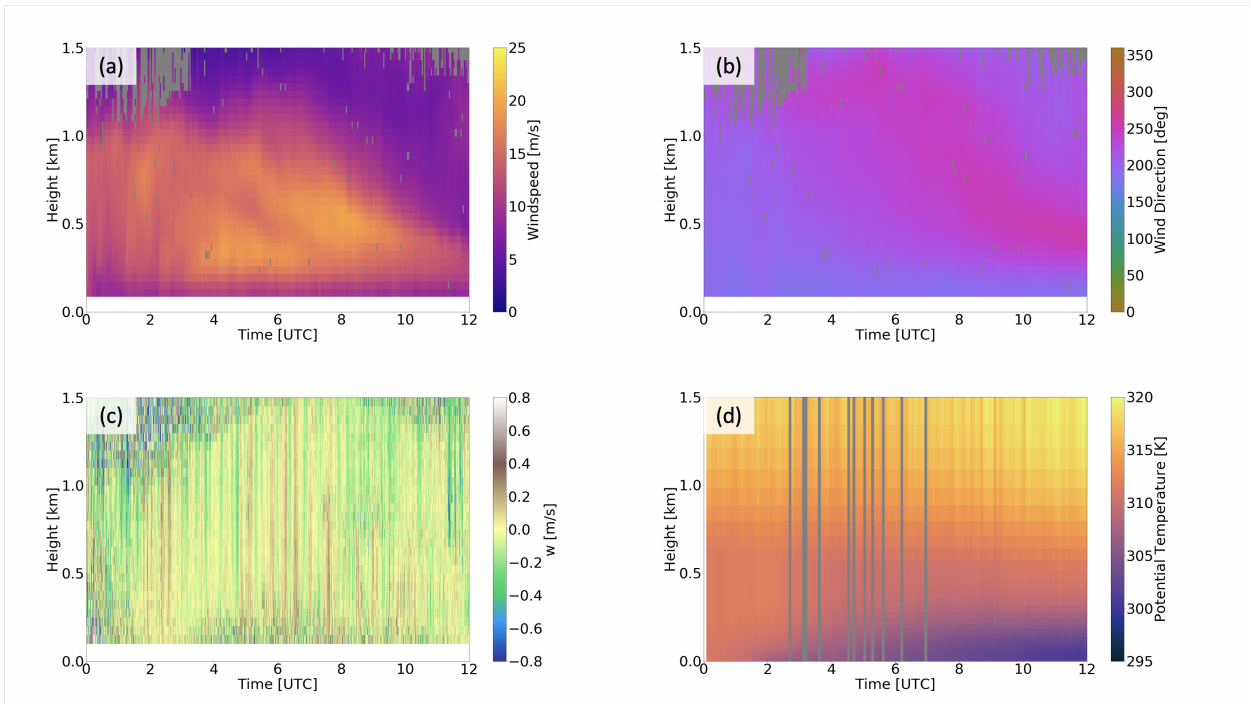


FIG. 17. Time-height cross sections of wind speed (a), wind direction (b), vertical velocity (c), and potential temperature (d) during IOP 27 at FP6.

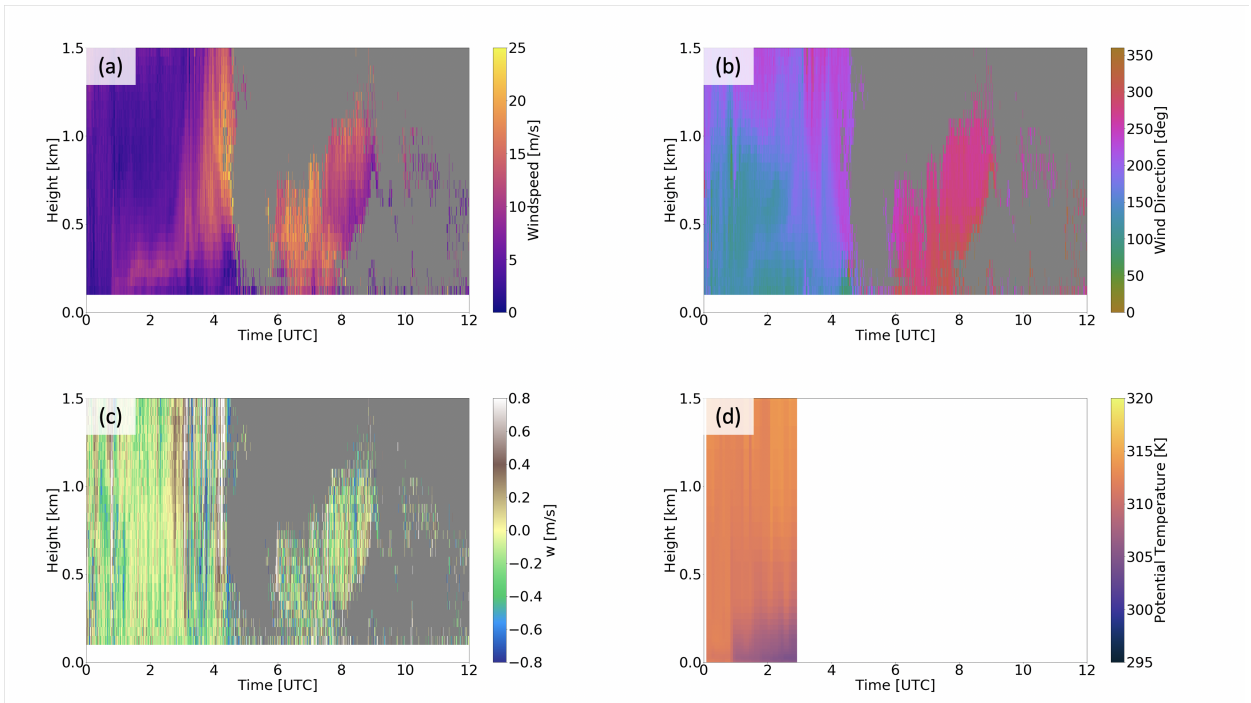


FIG. 18. Time-height cross sections of wind speed (a), wind direction (b), vertical velocity (c), and potential temperature (d) during IOP 31 at FP3.

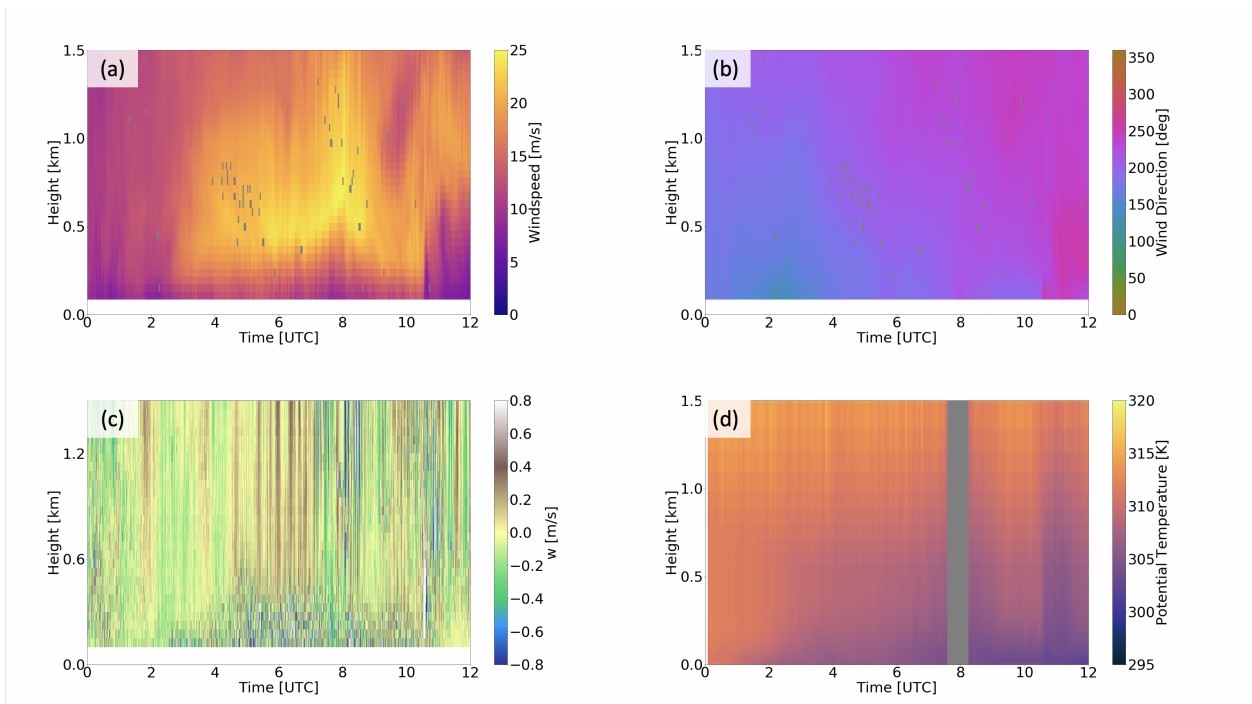


FIG. 19. Time-height cross sections of wind speed (a), wind direction (b), vertical velocity (c), and potential temperature (d) during IOP 31 at FP6.

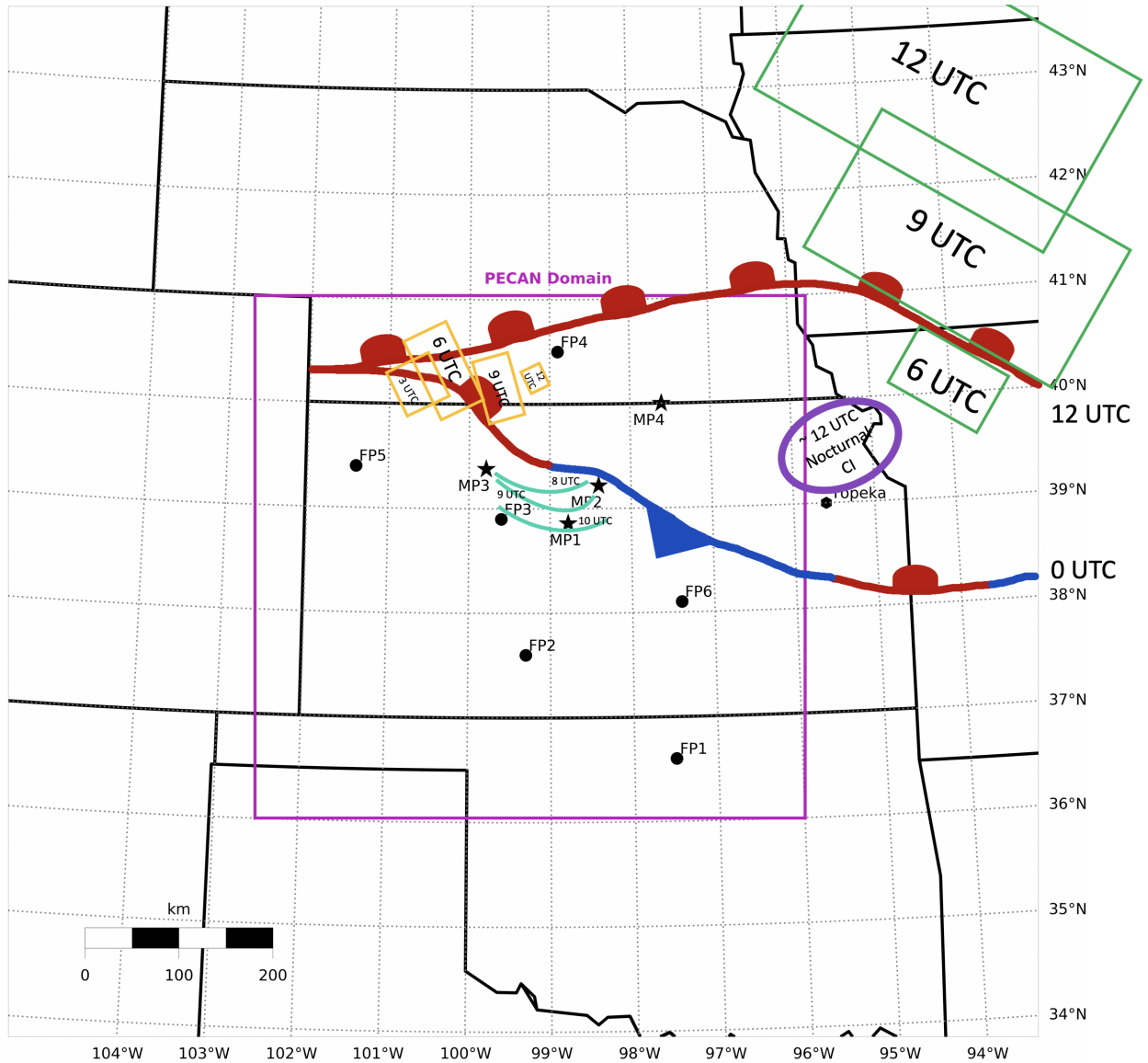


FIG. 20. PECAN domain depicting large scale features throughout the night on IOP 25. Areas of convection outlined in orange and green rectangles, nocturnal CI circled in purple, area of a bore-like structure in blue, and the locations of a stationary front (0 UTC) and warm front (12 UTC).

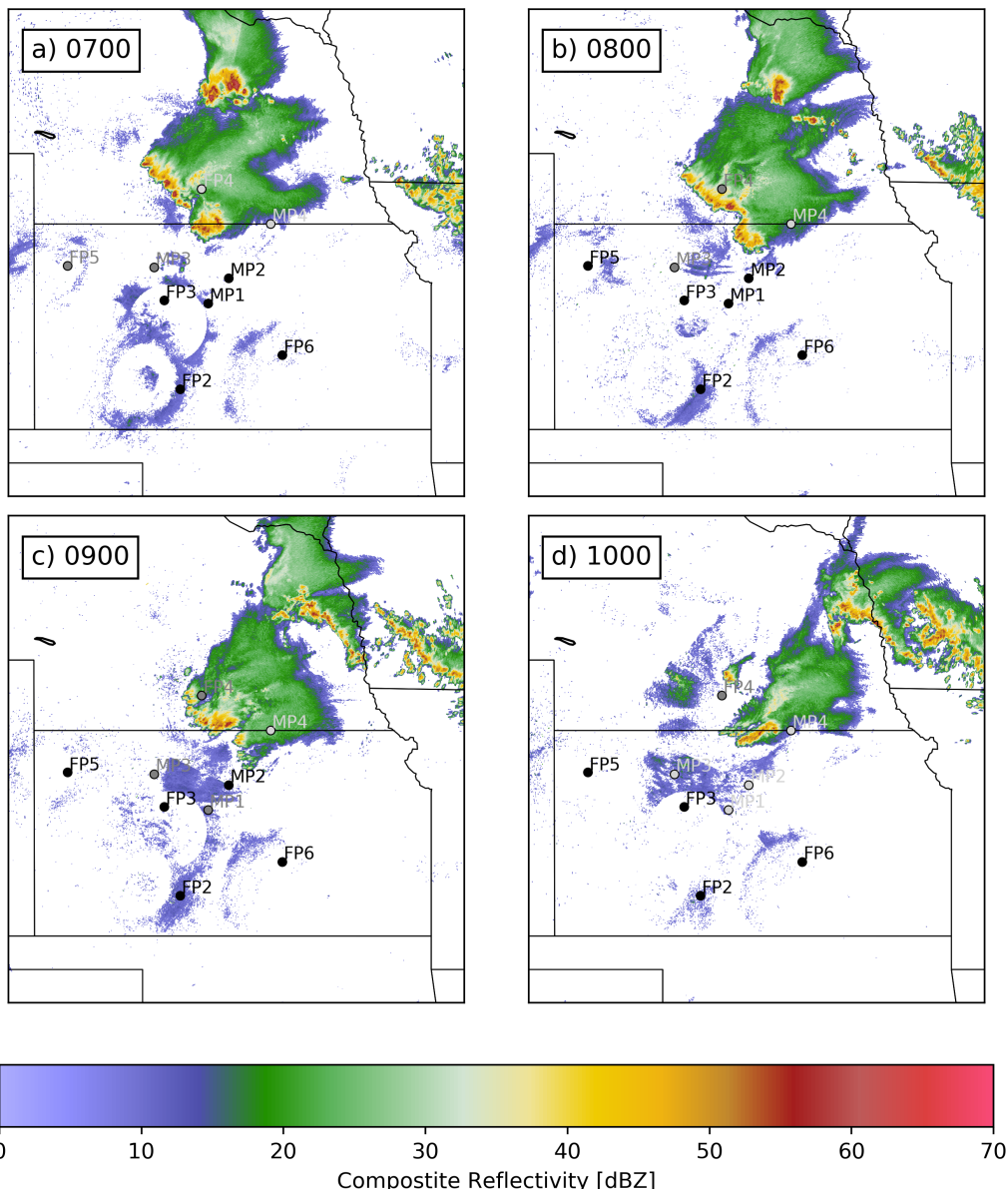


FIG. 21. Composite mosaic radar reflectivity on 11 July 2015 at (a) 0700, (b) 0800, (c) 0900, and (d) 1000 UTC.

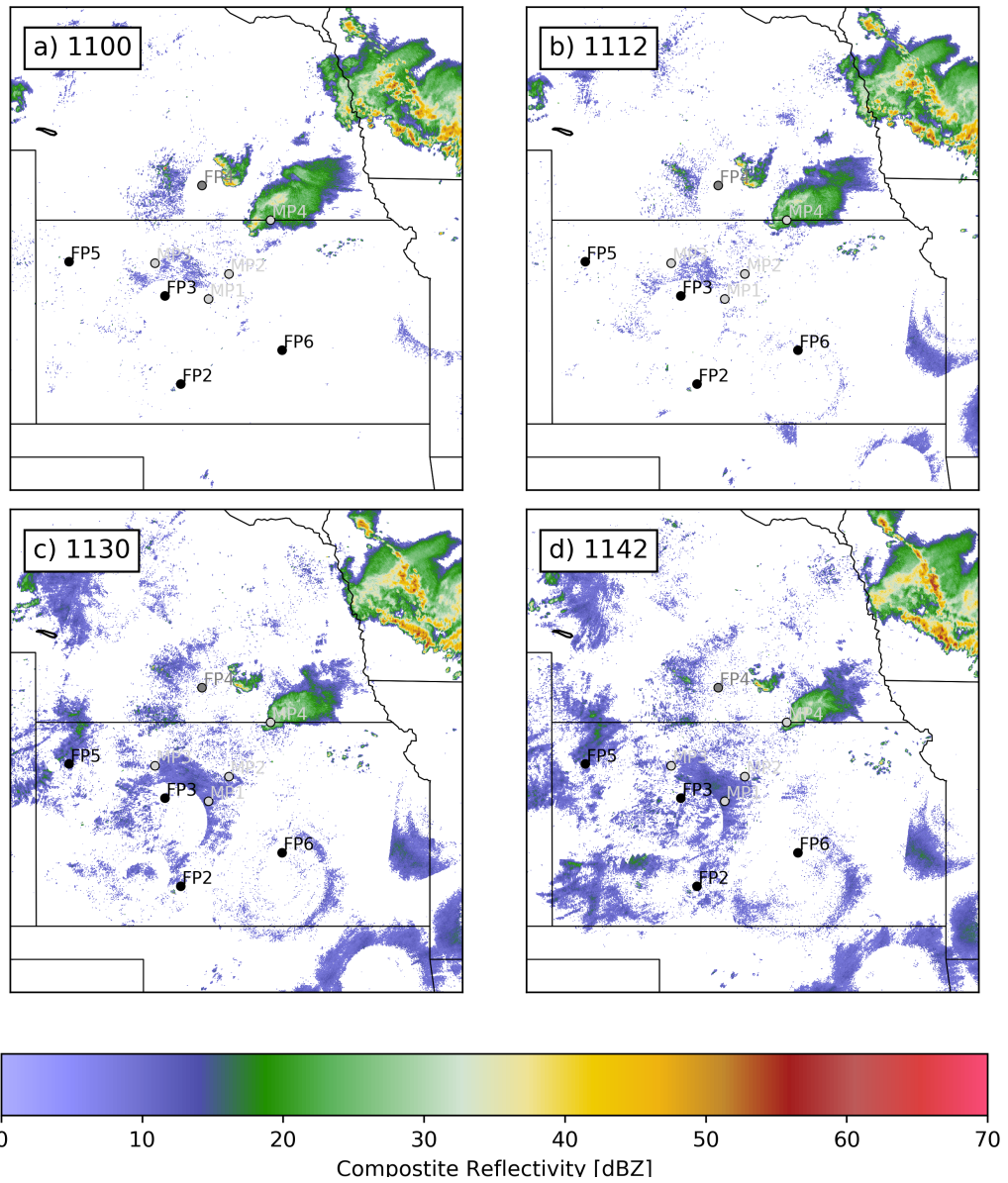


FIG. 22. Composite mosaic radar reflectivity on 11 July 2015 at (a) 1100, (b) 1112, (c) 1130, and (d) 1142 UTC.

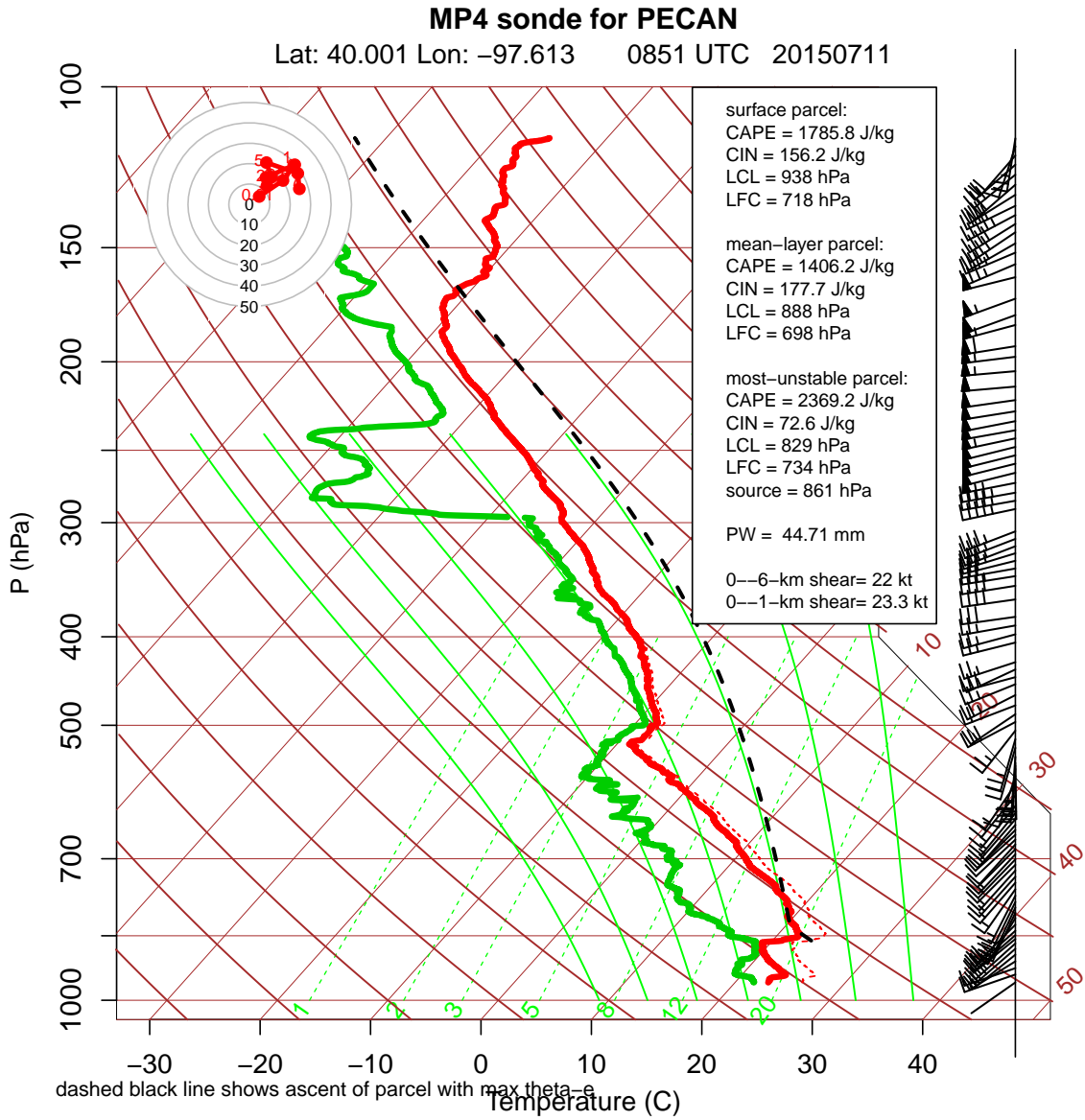


FIG. 23. MP4 sounding during IOP 25 launched at 0851 UTC.

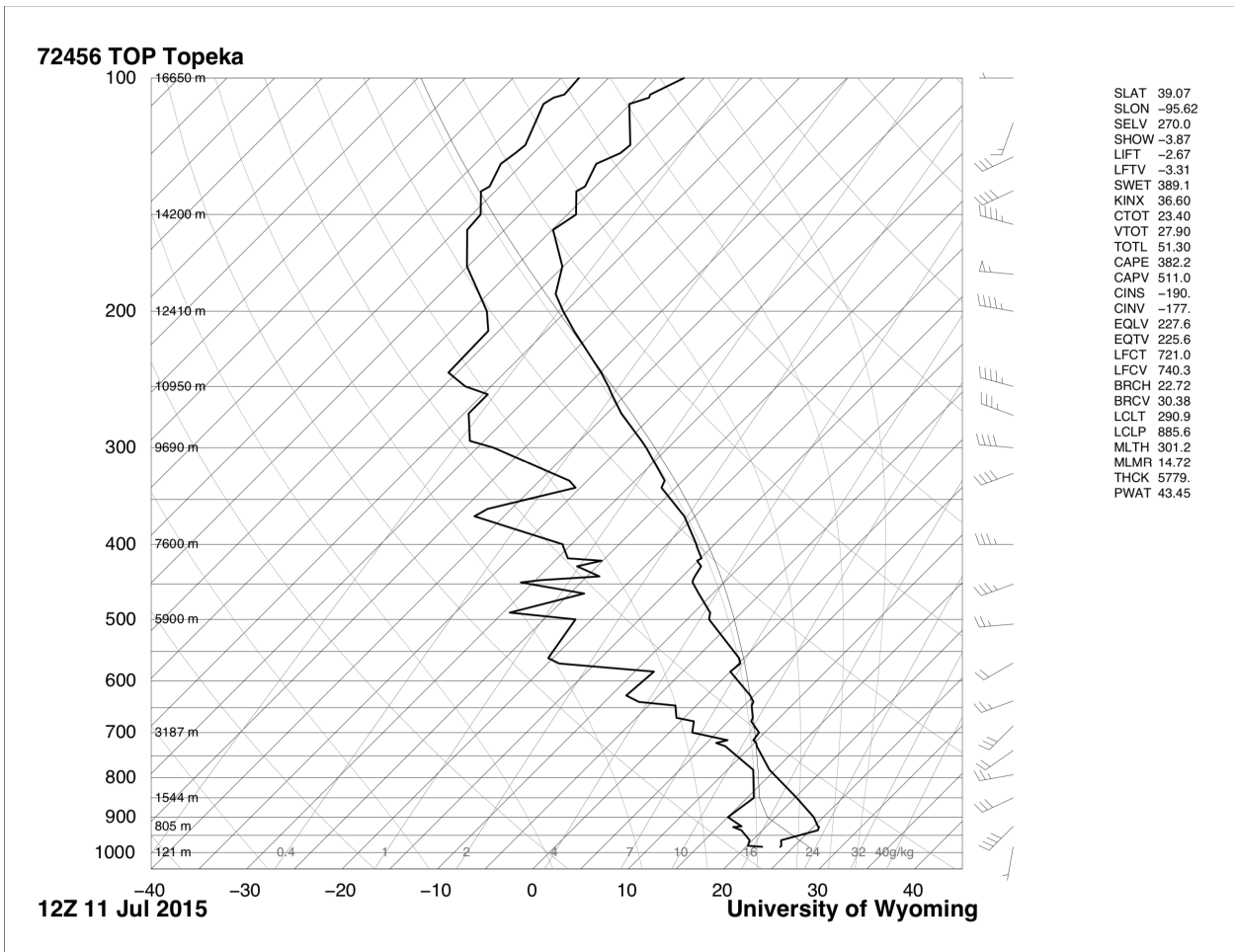


FIG. 24. Operational sounding from Topeka, KS during IOP 25 launched at 12 UTC